Turk J Elec Eng & Comp Sci
() : –

doi:10.3906/elk-

Channel Estimation for OFDM-IM Systems

Yusuf Acar[1,2*], Sultan Aldırmaz Çolak[3] , and Ertuğrul Başar[4]
[1]Department of Electrical and Electronics Engineering,
Istanbul Kultur University, 34156, Bakirkoy, Istanbul, Turkey.
[2]Wireless Technology Center, Purdue University-Fort Wayne, USA.
[3]Department of Electronics and Communication Engineering,
Faculty of Engineering, Kocaeli University, 41380, Kocaeli, Turkey.
[4]Communications Research and Innovation Laboratory
(CoreLab), Koç University, Department of Electrical and Electronics Engineering, Sarıyer 34450, Istanbul, Turkey.

Received: .201 • **Accepted/Published Online:** .201 • **Final Version:** ..201

Abstract:

Orthogonal frequency division multiplexing with index modulation (OFDM-IM) has been recently proposed to increase the spectral efficiency and improve the error performance of multi-carrier communication systems. However, all existing OFDM-IM systems assume that the perfect channel state information (P-CSI) is available at the receiver. Nevertheless, channel estimation is a challenging problem in practical wireless communication systems for coherent detection at the receiver. In this paper, a novel method based on pilot symbol aided channel estimation (PSA-CE) technique is proposed and evaluated for OFDM-IM systems. Pilot symbols, which are placed equidistantly, allow the regeneration of the response of channel so that pilot symbol spacing can fulfill the sampling theorem criterion. Our results shows that the low-pass interpolation and SPLINE techniques perform the best among all the channel estimation algorithms in terms of bit error rate (BER) and mean square error (MSE) performance.

Key words: Channel estimation (CE), orthogonal frequency division multiplexing (OFDM), indices modulation (IM), frequency selective fading channel, interpolation.

1. Introduction

Orthogonal frequency division multiplexing (OFDM) is a backbone of many wireless communications standards such as IEEE 802.16, WiMAX and LTE; furthermore, it has been also adopted for both up-link and down-link of 5G New Radio. One of the most important reasons for the preference of OFDM is its property of converting frequency selective channel into flat fading effectively by dividing wideband into smaller subbands. Another popular technique, multi-input multi-output (MIMO) transmission, has a major role in 4G (LTE) systems. In an LTE system, MIMO and OFDM are used together in order to increase data rate. However, this data rate does not seem to be sufficient for next generation systems along with the high transceiver complexity. To provide low cost implementation and high spectral efficiency, Mesleh *et al.* proposed the scheme of spatial modulation (SM) [1]. SM uses active antenna indices to transmit bits in addition to conventional modulations. SM can be considered as a low complexity alternative to conventional MIMO transmission schemes [1]. By using this technique, some drawbacks of the conventional MIMO systems, such as operation with multiple radio

*Correspondence: y.acar@iku.edu.tr, acary@pfw.edu

frequency chains, inter-antenna synchronization (IAS) at the transmitter and inter-channel interference (ICI) at the receiver, can be circumvented [2], [3].

Recently, Basar *et al.* have proposed the OFDM-IM scheme [5]. OFDM and SM schemes have been brought together into this technique, maintaining the properties of both. Similar to the use of active antenna indices for extra bit transmission in SM, OFDM-IM also uses indices of subcarrier locations to transmit data. Thus, average bit error probability (ABEP) of OFDM-IM under frequency selective channels is better than the classical OFDM [6, 7]. Furthermore, it requires less power compared to OFDM under the same spectral efficiency to achieve a target error rate. The use of indices for transmission adds a new dimension (third dimension) to the two-dimensional signal space. One of the main contributions of OFDM-IM system is the use of subcarrier indices as a data source. For this reason, OFDM-IM appears as a promising next-generation wireless communication technique, which offers a balanced trade-off between system performance and spectral efficiency compared to the classical OFDM system. OFDM-IM has attracted tremendous attention in the past few years. Interested readers are refered to [6, 7] and the references therein for an overview of the most recent developments.

Despite its advantages aforementioned, there are still problems in the practical application of OFDM-IM in wireless communications. The OFDM-IM receiver has to detect both the transmitted symbol and the indices of active subcarriers. In [5], detection both of active subcarriers indices and symbols are realized by using maximum likelihood (ML) and log likelihood ratio (LLR) detection methods under the assumption that the receiver has perfect channel state information (P-CSI). However, this assumption is impossible for practical systems, even if high computational complexity channel estimation techniques are used at the receiver. Consequently, there would be always a performance gap between the practical case and the P-CSI assumption. Therefore, channel estimation is an essential process at the practical OFDM-IM receiver during the coherent detection of the transmitted symbols and the active subcarrier which are, randomly selected. To reduce the performance gap, channel estimation techniques with low computational complexity should be developed. Recently, channel estimation has been comprehensively studied in the literature for SM based systems [8–10]. However, to the best of our knowledge, channel estimation problem of the OFDM-IM has not been studied in the literature yet.

In the literature, a considerable number of studies on channel estimation for the OFDM system, particularly comb-type based structures, can be found. The pilot assisted channel estimation (PSA-CE) has been generally performed for coherent detection performance in wireless environments and has been adapted in various communication systems, such as LTE-Advanced and WIMAX systems [11, 12]. However, when the indices of the subcarriers activated according to the corresponding information bits, pilot symbol sequence cannot be effective to implement channel estimation efficiently. Therefore, these techniques cannot be applicable directly to OFDM-IM due to subcarrier activation that depends on the indices bits. In this paper, we propose a new PSA-CE technique with interpolation for OFDM-IM systems according to activated subcarriers. First, pilot symbols are inserted having regard to activated subcarriers in the frequency domain to track the variation of the channel in the frequency domain. Then, one of the interpolation techniques, such as nearest interpolation (NI), piecewise linear interpolation (PLI), piecewise cubic Hermite (PCHIP, SPLINE), FFT interpolation (FFTI) and low-pass interpolation (LPI), are performed to estimate the channel frequency responses at data symbols. With extensive computer simulations, it is demonstrated that the LPI and SPLINE techniques perform the best among all the channel estimation algorithms in terms of bit error rate (BER) and mean square error (MSE) performance. Moreover, classical OFDM results are given as a benchmark. It is shown that OFDM-IM is more robust to channel estimation errors than classical OFDM systems.

The main contributions of the paper are summarized as follows:

- In the literature, most of the studies on OFDM-IM present the performance of their system assuming that the receiver has P-CSI. However, this assumption is not practical. To assess the real performance of the OFDM-IM system, channel estimation is indispensable. This paper analyzes this problem for the first time in the literature.
- BER performance of different interpolation techniques, such as NI, PLI, PCHIP, SPLINE, FFTI and LPI, is investigated for the OFDM-IM system.
- MSE performance of the aforementioned interpolation techniques is investigated for the OFDM-IM system.

The paper is organized as follows. Section 2 provides some essential information on OFDM-IM systems and the detection process. Section 3 gives a short overview about channel estimation for the OFDM-IM system. Section 4 provides brief information about interpolation techniques. Then the proposed pilot assisted channel estimation is investigated. Computer simulation results are given and discussed in Section 5. Finally our paper concludes in Section 6.

Notation: Throughout the paper, the following notation and assumptions are used. Small and bold letters '**a**' denote vectors. Capital and bold letters '**A**' denote matrices. $(.)^T$, $(.)^H$, $\|.\|$ and $(.)^{-1}$ denote transpose, Hermitian transpose, Euclidean norm and inverse of a vector or a matrix, respectively. S denotes the complex signal constellation of size M. The probability density function (PDF) of the random variable (r.v.) X denoted by $p_X(x)$ and $E\{X\}$ represents expectation of the r.v. X.

2. Orthogonal frequency division multiplexing-index modulation (OFDM-IM)

2.1. Signal model

In this paper, we analyze an OFDM-IM system operating over a frequency-selective Rayleigh fading channel. The data structure of the classical OFDM symbol and OFDM-IM symbol is given in Fig. 1 and the parameters of the OFDM-IM scheme are summarized in Table 1.

In the OFDM-IM scheme, the total transmitted bits are split into g subblocks and there are index selectors and mapping blocks for each subblock. Then, at each subblock β, indices are selected by using the incoming p_1 bits at the index selector. The selected indices are given as $I_\beta = \{i_{\beta,1} \cdots i_{\beta,k}\}$ where $i_{\beta,\gamma} \in [1, \ldots, n]$ for $\beta = 1, \ldots, g$ and $\gamma = 1, \ldots, k$. The data symbols at the output of the M-ary modulator, which are determined by p_2 bits, are given as $\boldsymbol{s}_\beta = [s_\beta(1) \cdots s_\beta(k)]$ where $s_\beta(\gamma) \in S, \beta = 1, \ldots, g, \gamma = 1, \ldots, k$. By using I_β and s_β for all β, the OFDM block generator creates all of the subblocks and then creates $N \times 1$ OFDM-IM symbol as $\boldsymbol{x}_F = [x(1) \cdots x(N)]^T$ where $x(\alpha) \in \{0, S\}, \alpha = 1, \ldots, N$. The OFDM-IM symbol contains some zero terms whose positions carry information unlike the conventional OFDM.

Transmission frequency-selective channel is assumed as a Rayleigh fading channel whose channel coefficients can be written as

$$\boldsymbol{h}_T = [h_T(1) \cdots h_T(d)]^T \tag{1}$$

whose elements have distribution $\mathcal{CN}(0, \frac{1}{d})$ and d is the length of the channel impulse response (CIR). At the trasmitter, after IFFT operation, cyclic prefix (CP) is added to the output of the IFFT. Then OFDM-IM signal is sent over the channel $\boldsymbol{h}_T$.

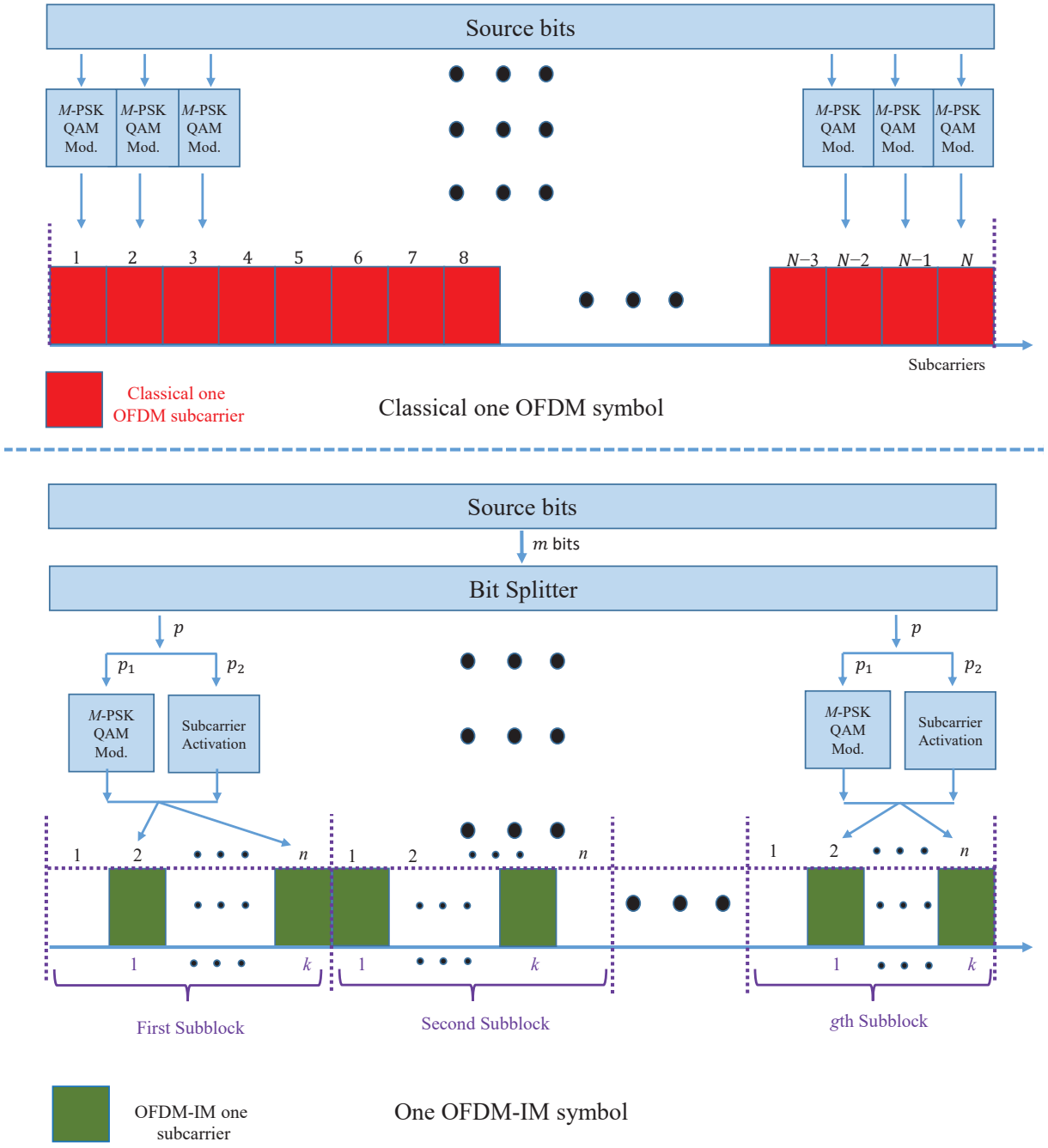

Figure 1. Data Frame Structure of Conventional OFDM and OFDM-IM

Table 1. OFDM-IM Parameters

Parameters	Definition
g	Number of subblocks
m	Total number of information bits for OFDM-IM symbol
p	Number of bits transmitted in each subblock (i.e., $p = m/g$)
N	Number of OFDM subcarriers (i.e., size of FFT)
n	OFDM-IM subblock length (i.e., $n = N/g$)
k	Number of activated subcarrier indices in each subbock
K	Total number of active subcarriers (i.e., $K = kg$)
p_1	Total number of bits that are mapped onto the active indices in each subbock
p_2	Total number of bits that are mapped onto the M-ary signal constellation

At the receiver, after using an A/D converter and removing CP, fast Fourier transform (FFT) is applied to the received OFDM-IM symbol. The received frequency domain OFDM-IM symbol can be written for fth subcarrier as follows:

$$y_F(f) = h_F(f)x(f) + w_F(f), \quad f = 1, ..., N \tag{2}$$

where $w_F(f)$ and $h_F(f)$ are the frequency-domain noise samples and channel fading coefficients with distributions $\mathcal{CN}(0,1)$ and $\mathcal{CN}(0, \left(\frac{K}{N}\right) W_{0,T})$, respectively, and $W_{0,T}$ is the time domain noise variance.

2.2. Detection in OFDM-IM system

In the OFDM-IM scheme, the receiver should detect the indices of the active subcarriers besides the information bits carried by the M-ary symbols. In [5], ML and LLR detectors have been proposed. The ML detector performs all subblock realizations by considering a search for all transmitted symbols and subcarrier index combinations as follows

$$\left(\hat{I}_\beta, \hat{s}_\beta\right) = \arg \min_{I_\beta, s_\beta} \sum_{\gamma=1}^{k} \left| y_F^\beta(i_{\beta,\gamma}) - h_F^\beta(i_{\beta,\gamma}) s_\beta(\gamma) \right|^2 \tag{3}$$

where $y_F^\beta(\xi) = y_F(n(\beta-1)+\xi)$ and $h_F^\beta(\xi) = h_F(n(\beta-1)+\xi)$ are the corresponding fading coefficients and received signals, respectively.

It is shown that the complexity of ML decoding increases for higher n and k values [5]. To reduce the encoder/decoder complexity, in this work, a LLR algorithm is utilized at the receiver to decide the most likely corresponding data symbols and active subcarriers. It determines the logarithm of the ratio of a posteriori probabilities of OFDM samples for each subcarrier. This ratio is given as

$$\lambda(f) = \ln \frac{\sum_{\chi=1}^{M} P(x(f) = s_\chi \,|y_F(f))}{P(x(f) = 0 \,|y_F(f))} \tag{4}$$

where $s_\chi \in S$. As seen from (4), the higher value of $\lambda(f)$ indicates that the fth subcarrier is more likely to be active. Finally, active indices and symbols are then passed to the demapper to retrieve the original information. As a result, in (3) and (4), the indices of the active subcarriers and symbol detection are performed under the assumption that P-CSI is known at the receiver. However, it is challenging to obtain P-CSI for practical systems. Therefore, channel estimation is an important and essential process at the practical OFDM-IM receiver for the coherent detection of s_β and I_β.

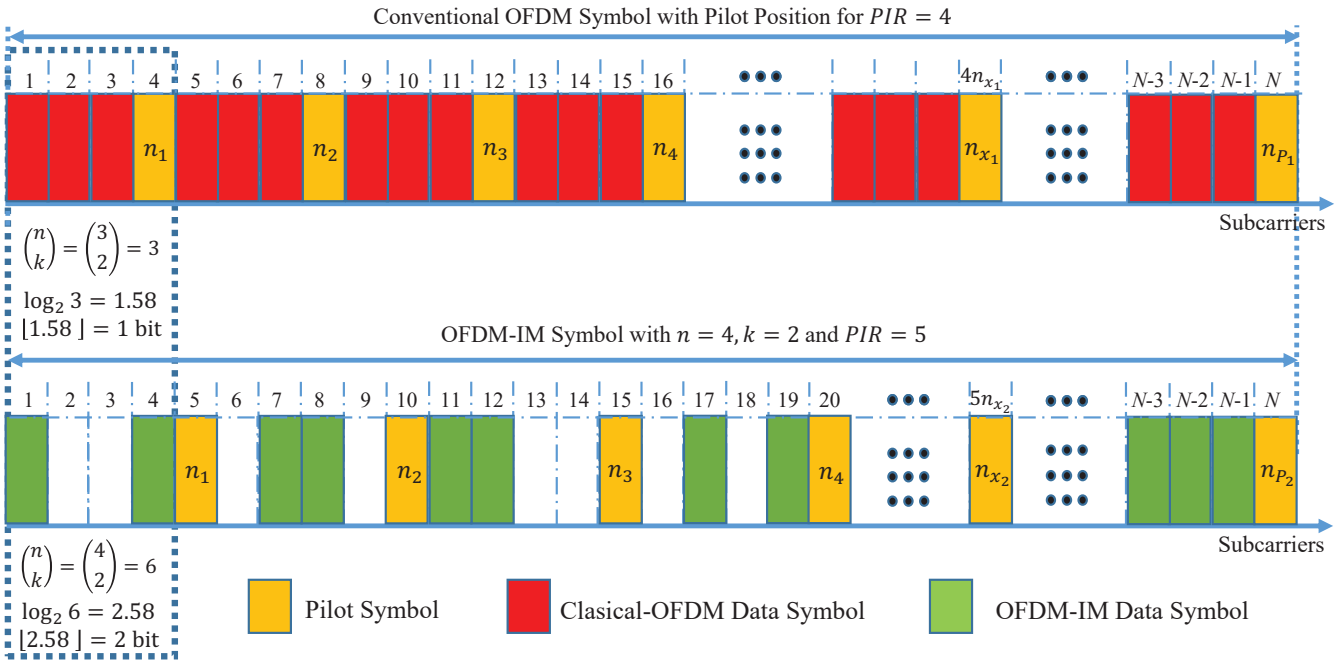

Figure 2. Pilot Frame Structure of Conventional OFDM and OFDM-IM for $n = 4$ and $k = 2$

3. Channel estimation for the OFDM-IM system

Generally, wireless communications systems expose to frequency selective fading channel due to the multipath propagation. Therefore, the channel may be destructive for the transmitted signal. To compensate the channel effects, the channel frequency response should be estimated in the receiver side. Besides, systems such as OFDM-IM, need the channel frequency response at the receiver side for joint detection of the modulated symbols, s_β, and the subcarrier indices, I_β. However, to the best of our knowledge, channel estimation problems have not been extensively explored for OFDM-IM in the literature yet. In OFDM-IM systems, when the subcarriers are activated according to the associated data bits, pilot symbol sequence cannot be effectively implemented for channel estimation.

The top of Figs. 2-3 show the well known comp-type frame structure of conventional OFDM technique. In this figure, yellow, red and green items represent the pilot symbol, classical-OFDM data symbol and OFDM-IM data symbols, respectively. It is clear that conventional OFDM systems do not convey information bits over the subcarrier indices, hence, the positions of the pilots are not important at the transmitter and the pilots can be placed without any restriction. The bottom of these figures show the proposed frame structure for OFDM-IM systems. The main difference between these structures is that in the conventional OFDM system, all subcarriers are activated; however in OFDM-IM system, this is not the case. Hence, the positions of pilots become important for OFDM-IM systems as outlined in the following two scenarios:

***Scenario-1*:** As shown in the upper part of Fig. 2, in the classic OFDM, when pilot insertion ratio (PIR) is selected as 4, pilot data is inserted into each fourth subcarrier and the pilot positions are defined as $4 - 8 - 16 - ... - N$. If the same structure is used for OFDM-IM, $C(3, 2) = 3$ different combinations can be obtained for a subblock length of $n = 4$ and the number of active subcarriers is selected as $k = 2$. By this way, we can transmit 1.58 bits for 3 different selections as an index bit, i.e., a maximum of 1 bit will be assigned

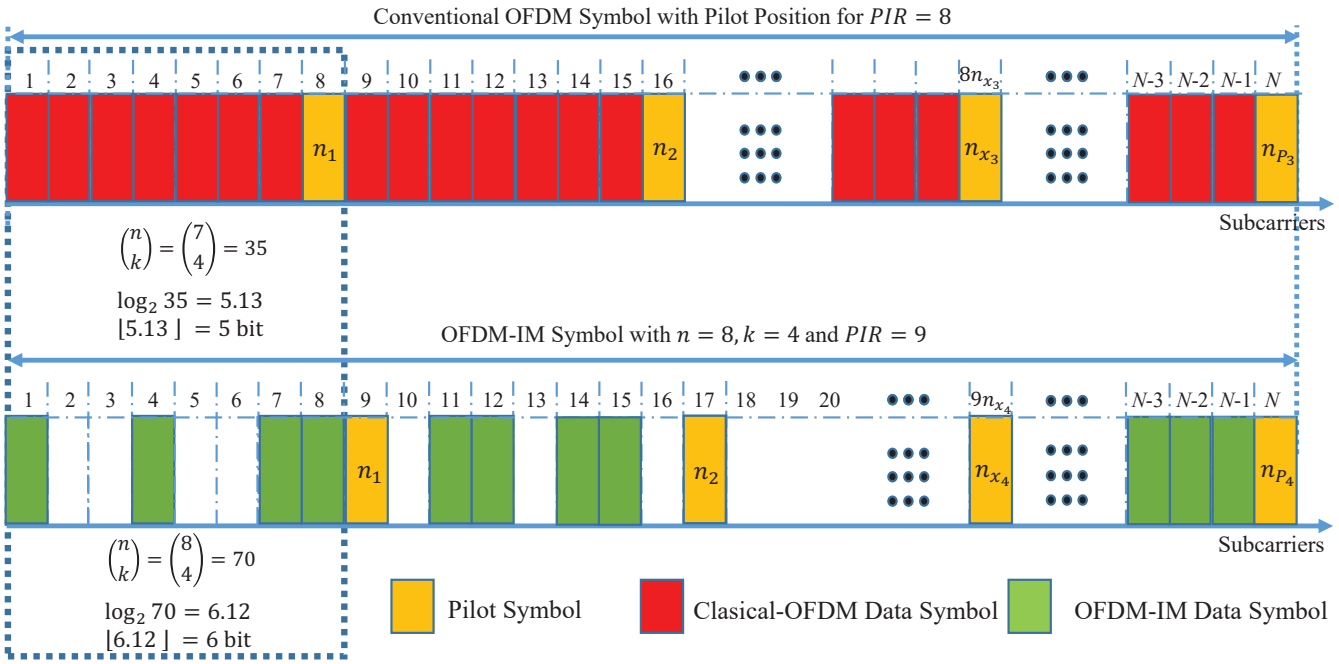

Figure 3. Pilot Frame Structure of Conventional OFDM and OFDM-IM for $n = 8$ and $k = 4$

for subcarrier indices. In this study, considering different subblock lengths (n) and active subcarriers (k) for OFDM-IM, pilot positions are determined. As seen at the bottom of Fig. 2, the pilots are inserted after the subblocks and 6 different combinations are obtained from $C(4, 2)$. In this manner, 2 bits are assigned as index bits, and the spectral efficiency of the proposed technique can be increased.

***Scenario-2*:** Similar to *Senario-1*, when PIR is selected as 8 in the classic OFDM, pilots are inserted into $8 - 16 - 32 - ... - N$ subcarriers as shown in Fig. 3. In this case, if the number of active subcarriers is selected as $k = 4$, there will be 35 different options ($C(7, 4)$) whereas with the proposed scheme, there will be 70 different options ($C(8, 4)$). Hence, 6 bits can be transmitted via indices instead of 5 bits. In addition, the total number of pilots in classical OFDM n_{p_1} and n_{p_3} will be greater than n_{p_2} and n_{p_4} in OFDM-IM. Since less pilot symbols are used in OFDM-IM and also thanks to index bits, the efficiency increases compared to the that of the classical OFDM.

To obtain the frequency variation of the wireless channel, pilot symbols (where totally P pilot symbols are employed) are placed with equal distances in the frequency domain. Then, the received signals at pilot subcarriers can be expressed for each OFDM-IM symbol as follows:

$$y_F(n_p) = \psi h_F(n_p) + w_F(n_p), \quad n_p = 1, PIR + 1, ..., N \tag{5}$$

where ψ is the pilot symbol. After obtaining the received signal at the known pilot tone positions, the frequency response of channel at the pilot position can be estimated by using least square (LS) method as follows:

$$\widehat{h}(n_p) = y_F(n_p)/\psi. \tag{6}$$

Curve fitting or interpolation techniques can be used in the process of constructing the whole channel

response. In this paper, following interpolation techniques are used to estimate the channel variations at the data subcarriers by using the channel parameters in (6).

4. Interpolation techniques

In this paper, in order to track the selectivity of channels, we use suitable interpolation techniques. Hence, the channel variations at the data subcarriers are estimated by interpolation methods. Coleri *et. al.* have studied several interpolation techniques comparatively, and they showed that the LPI has advantages (favorable) compared to the others due to its superior performance [13]. In the following subsection, we give some brief information about different interpolation methods.

4.1. Piecewise linear interpolation (PLI)

Due to its inherent simplicity and easy implementation PLI is one of the most favorable interpolation method [14]. The PLI can be expressed for $p = 1, 2, \cdots, P$ as follows:

$$h(n) \;=\; \hat{h}(n_p)+\Big(\hat{h}(n_{p+1})-\hat{h}(n_p)\Big)\left(\frac{n-n_p}{D}\right), \text{for } n_p \le n \le n_{p+1} \tag{7}$$

where $\hat{h}(n_p)$ and $h(n)$ are the estimated CIRs at pilot positions and at all data positions, respectively.

4.2. Piecewise cubic hermite interpolation

The piecewise cubic polynomials are one of the powerful solutions for interpolation [15], [16]. (8) represents the Piecewise Cubic Hermite Interpolation for the local variables $m = n - n_p$ on the interval $n_p \le n \le n_{p+1}$:

$$h(n)=\frac{3Dm^2-2m^3}{D^3}\hat{h}(n_{p+1})+\frac{D^3-3Dm^2+2m^3}{D^3}\hat{h}(n_p)+\frac{m^2(m-D)}{D^2}d_{p+1}+\frac{m(m-D)^2}{D^2}d_p \tag{8}$$

where d_p is the slope of the interpolant at n_p and D denotes the length of the subinterval. There are numerous approaches to assess both the function values and the first derivatives at the positions of a set of data points. Hence, the slope d_p should be calculated in a proper way. In what follows, we introduce the *pchip* and *spline* interpolation techniques to acquire piecewise cubic Hermite interpolation.

4.2.1. Shape-preserving piecewise cubic interpolation (PCHIP)

The PCHIP algorithm, determines the slopes d_p as follows [17],[18];

- Assume that $\delta_p = \frac{\hat{h}(n_{p+1})-\hat{h}(n_p)}{D}$ is the first-order difference of $\hat{h}(n_p)$.
- If δ_p and δ_{p-1} have opposite signs, set $d_p = 0$
- If δ_p and δ_{p-1} have zero or both of them have zero signs, set $d_p = 0$
- Otherwise, set the d_p as $d_p = \frac{2\delta_{p-1}\delta_p}{\delta_{p-1}+\delta_p}$.

4.2.2. Cubic SPLINE interpolation

The common property of PCHIP and this technique is their same interpolation constraints. Cubic SPLINE algorithm employs low-degree polynomials in each interval and selects the polynomial pieces. This technique is twice continuously differentiable. This interpolation method can calculate the d_p values as follows [19];

$$\mathbf{Bd} = \mathbf{r} \tag{9}$$

where $\mathbf{d} = [d_0, d_1, \ldots, d_{P-1}]^T$ is the slopes vector and $\mathbf{B}$ is a tridiagonal matrix

$$\mathbf{B} = \begin{bmatrix} A & 2A & & & & \\ A & 4A & A & & & \\ & A & 4A & A & & \\ & & \ddots & \ddots & \ddots & \\ & & & A & 4A & A \\ & & & & A & 4A \end{bmatrix}$$

and the right-hand side of (9) is $\mathbf{r} = 3\left[\frac{5}{6}A\delta_0 + \frac{1}{6}A\delta_1, A\delta_0 + A\delta_1, \ldots, A\delta_{P-3} + A\delta_{P-2}, \frac{1}{6}A\delta_{P-3} + \frac{5}{6}A\delta_{P-2}\right]^T$.

As a conclusion, the SPLINE interpolant is smoother than the PCHIP interpolant. While PCHIP has only first continuous derivatives that implies a discontinuous curvature, in addition to the first continuous derivatives, SPLINE also has second continuous derivative. On the other hand, contrary to PCHIP, SPLINE might not be protected to preserve the shape.

4.3. Low pass interpolation (LPI)

LPI technique is another method for the channel estimation [20]. For the calculation of the filter coefficients, LPI does not require the knowledge of the signal-to-noise ratio (SNR) as well as the autocorrelation function of the channel fading coefficients. Firstly, $Z-1$ zeros inserted between successive samples of $\hat{h}(n_p)$ with a sampling rate f_p, as:

$$\tilde{h}(n) = \begin{cases} \hat{h}(n_p) & n = 0 : Z : Z(P-1) \\ 0 & \text{otherwise.} \end{cases} \tag{10}$$

Then, to calculate the interpolated signal $h(n)$, (10) and the raised-cosine low pass filter $h_{LP}(n)$ with a cutoff frequency, specified by $f_c = \frac{\tilde{f}_p}{2Z} = \frac{f_p}{2}$ as given follows [21]:

$$h(n) = \sum_{n_p=-\infty}^{\infty} h_{LP}(n - n_p)\tilde{h}(n) \tag{11}$$

4.4. Fast Fourier transform interpolation (FFTI)

The FFT algorithm is an accurate and efficient method for interpolation and a well-known application of the FFT [22],[23]. This technique is also very effective by significantly reducing the noise on the estimated channel coefficients [24]. Fig. 4 shows the basic block diagram of the FFT interpolator. As shown in Fig. 4, after obtaining channel parameters at pilot tones sequence, FFT of $\hat{h}(n_p)$ is computed as $\hat{h}_{fft}(n_p)$. Secondly, the

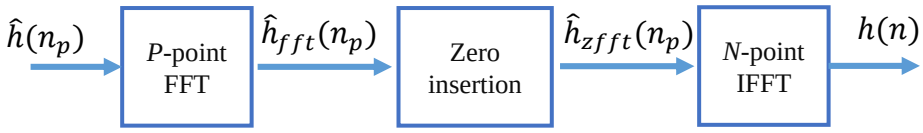

Figure 4. The block diagram of the FFT interpolator

null samples are added in $\hat{h}_{fft}(n_p)$ to obtain $\hat{h}_{zfft}(n_p)$. Finally, the inverse FFT (IFFT) is applied to the oversampled vector, $\hat{h}_{zfft}(n_p)$ to calculate the interpolated signal $h(n)$.

4.5. Zero-order hold or nearest interpolation (NI)

NI is one of the simplest interpolation techniques in which the value of the nearest point is selected. To calculate the interpolated signal $h(n)$, (10) is convolved with $h_Z(n)$ as given in the following, where $h_Z(n)$ is equal to 1 for $0 \leq n \leq Z$ and zero otherwise:

$$h(n) = \sum_{n_p=-\infty}^{\infty} h_Z(n - n_p)\tilde{h}(n_p) \tag{12}$$

where Z denotes the length of the subinterval.

5. Simulation results

The BER and MSE performance of OFDM-IM systems is evaluated by employing OFDM-IM with different N, k and n parameters under frequency selective Rayleigh channels. Monte Carlo simulations are performed by employing BPSK, QPSK, 8-QAM and 16-QAM signal constellations. Moreover, we present channel estimation results for classical OFDM systems in order to compare the performance of OFDM-IM systems. In all computer simulations, we assumed the following system parameters: $d = 10$ and a CP length of $L = 16$. SNR is defined as E_s/N_0, where E_s is energy per symbol and N_0 is the noise power. At the receiver, a LLR detector is used for detection process.

In Fig. 5, the BER performance of the proposed channel estimation methods with interpolation techniques are compared for the BPSK signaling with $n = 4$, $k = 2$ and $PIR = 5$ where PIR is pilot insertion rate. As seen from of Fig. 5*a*, for $N = 128$, all interpolation based channel estimation techniques have an irreducible error floor at high SNR values. To overcome this problem PIR might be decreased however, the overhead increases in this case, and the spectral efficiency of the OFDM-IM decreases due to the reduced number of active subcarrier combinations. Therefore, in Fig. 5*b*, we increased the total number of the subcarrier to $N = 256$. It is observed that SPLINE slightly outperforms the FFTI while it shows a similar performance to LPI for the scheme with $N = 256$, $n = 4$, $k = 2$ and $PIR = 5$. Moreover, SPI and LPI exhibit a detection gain of about 6 dB over PCHIP at a BER value of 10^{-4}. It is also demonstrated that NI, LI and PCHIP have an irreducible error floor at high SNR. According to the selected parameters, there will be 64 subblocks in OFDM-IM. Because 2 bits are conveyed by the indices of the subcarriers, total number of the transmit index bits equals to 128 bits. In addition to index bits, 2 bits in each subblocks are conveyed via active subcarriers. Hence in one OFDM-IM symbol, we can transmit 256 bits. In the classical OFDM symbol, 256 bits (same

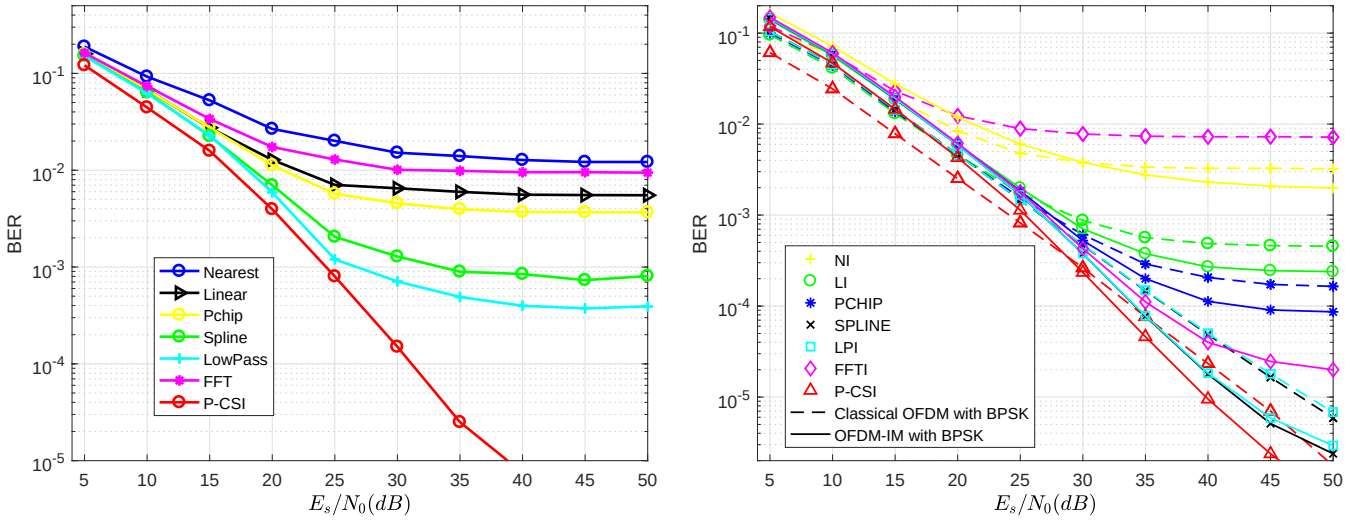

(a) (b)

Figure 5. The BER performance of OFDM-IM with BPSK, $n = 4$, $k = 2$, $PIR = 5$ (a) $N = 128$ (b) $N = 256$

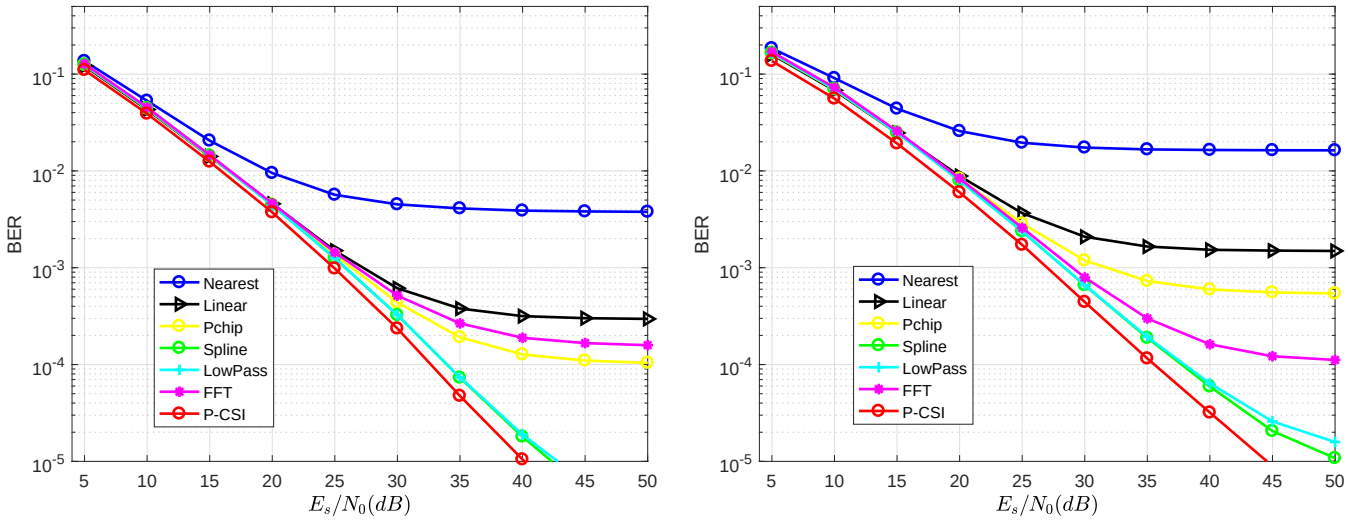

(a) (b)

Figure 6. The BER performance of OFDM-IM with $n = 4$, $k = 2$, $PIR = 5$, $N = 256$ (a) QPSK (b) 8-QAM

as OFDM-IM scheme) are transmitted when all subscarriers are active and BPSK is used. Although achieving the same SE is achieved by both these techniques, it is shown from Fig. 5 that OFDM-IM is more robust to channel estimation errors than classical OFDM systems.

BER performance results of the QPSK and 8-QAM signaling, with $n = 4$, $k = 2$, $PIR = 5$, $N = 256$, are plotted in Fig. 6 as a function of the SNR. In Fig.6*a*, the SPLINE and the LPI have the same BER performances and they perform better than the other interpolation based channel estimation techniques. It is

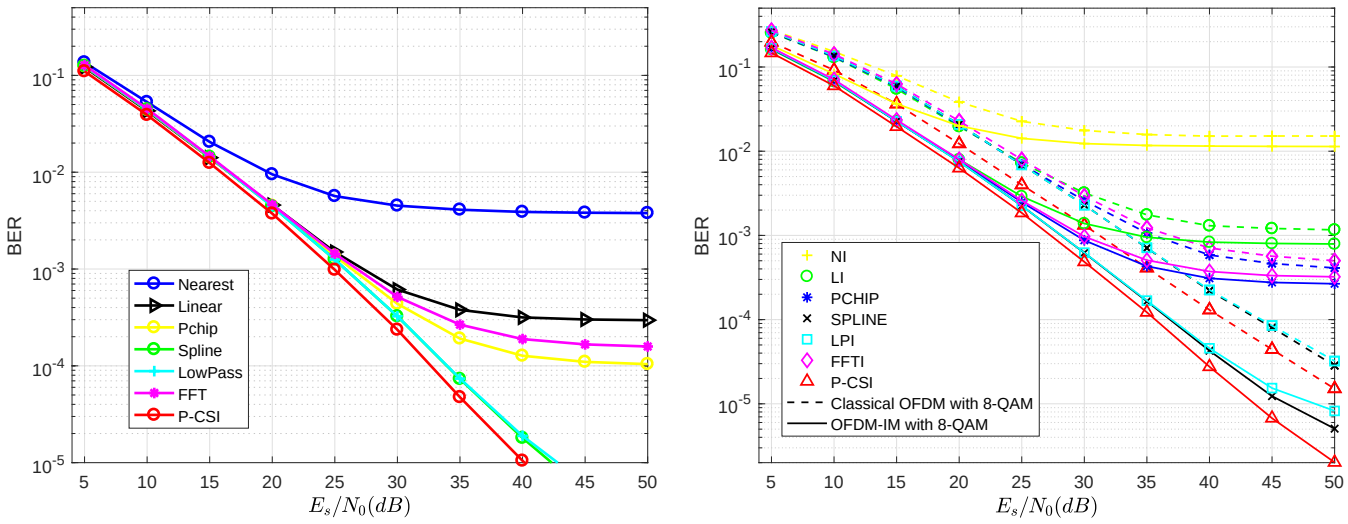

Figure 7. The BER performance of OFDM-IM with $n = 8,\ k = 2,\ PIR = 9,\ N = 512$ (a)QPSK (b)8QAM

also shown that NI, PLI, PCHIP and FFTI based channel estimation methods have an irreducible error floor at high SNR. The superiority in performance of the SPLINE interpolation over the LPI is illustrated in Fig. 6*b* at high SNR for 8-QAM signaling. It is seen from Fig.6*b* that the SPLINE and the LPI exhibit a detection gain of about 8 dB over the FFTI at a BER value of 10^{-4}.

Pilot overhead is one of the problems faced in the receiver design. It decreases efficiency and data rate of systems. To overcome this problem, we decrease the number of the pilot symbols, i.e., we increase PIR. In Fig. 7, the BER performances of the proposed channel estimation methods with interpolation techniques are compared for QPSK and 8-QAM signaling with $n = 8,\ k = 2$ and $PIR = 9$. The BER performances of the channel estimation algorithms based on SPLINE and LPI are considerably better than NI, LI, PCHIP and FFTI algorithms, while these also yield error floor at high SNRs. In particular, in Fig. 7*b*, it is observed that LPI and SPLINE exhibit a detection gain of about 4 dB compare to PCHIP at a BER value of 10^{-3}. In Figure 7, it is assumed that $8-$QAM is used in OFDM-IM while BPSK is employed in the classical OFDM. According to this case (scenario), there will be 64 subblocks in OFDM-IM. Thus, 4 bits ($C(8,2)$) are conveyed by the indices of the subcarriers. Total number of the transmit index bits equals to 256 bits. In addition to index bits, we also use 8-QAM and transmit 6 bits in each subblocks for active subcarriers equals to 2 ($k = 2$). Hence in one OFDM-IM symbol, we can transmit 640 bits. In the classical OFDM, even if all subcarriers are active, only 512 bits are transmitted by using BPSK. Although OFDM-IM provides higher SE, it is seen that it performs much better than classical OFDM.

One of the important issues in wireless communications systems is the bandwidth efficiency. In [25], it has been demonstrated that the QAM is very sensitive to channel estimation errors and the performance degradation of a higher order QAM signaling scheme such as 16-QAM is more serious than that of lower order QAM signaling scheme. In Fig. 8, the effect of channel estimation on the BER performance of OFDM-IM for 16-QAM with $n = 4,\ k = 2$ and $PIR = 9$ plotted. In Fig. 8*a*, it is shown that the NI, PCHIP, PLI and FFTI experience severe performance degradation at higher SNR values compared to Fig. 7 because of higher

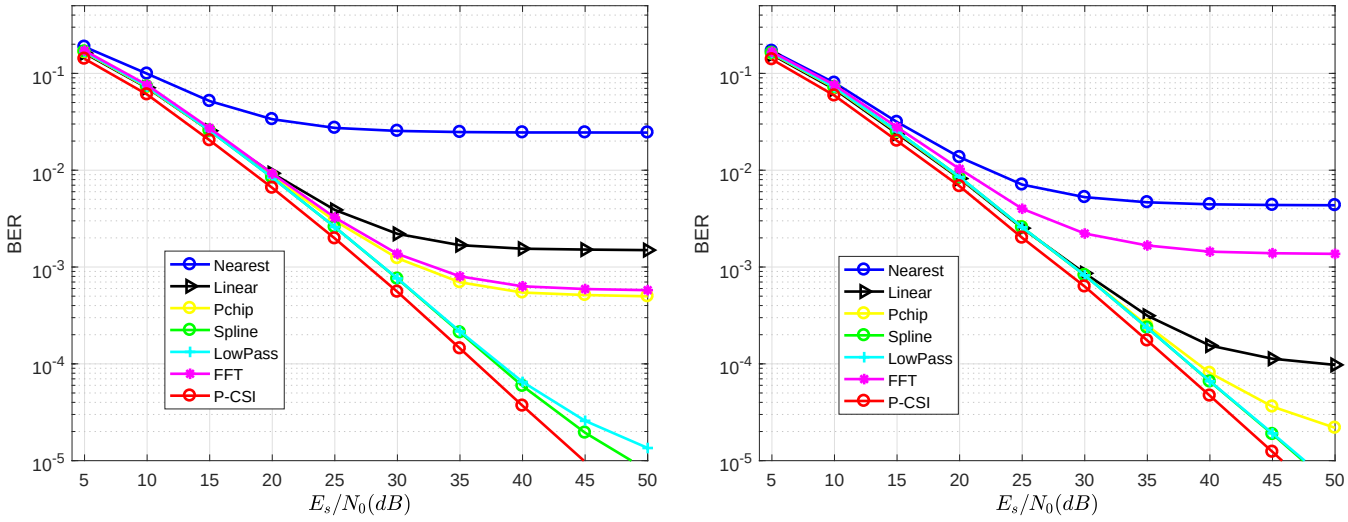

Figure 8. The BER performance of OFDM-IM with 16QAM, $n = 8$, $k = 2$, $PIR = 9$ (a) $N = 512$ (b) $N = 1024$

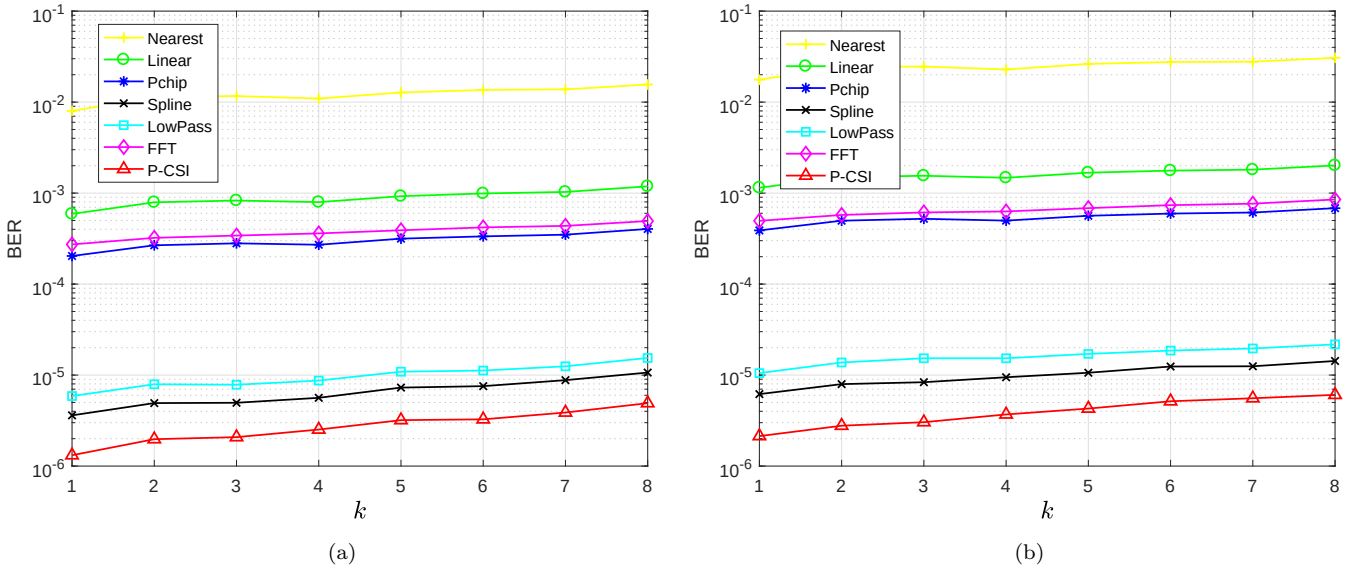

Figure 9. The BER performance of OFDM-IM with $SNR = 50$dB, $n = 8$, $PIR = 9$ (a) 8QAM (b) 16QAM

order QAM scheme. On the other hand, we increase the number of the subcarriers as $N = 1024$ in Fig. 8*b*. It is observed that the BER performance of the SPLINE and LPI based channel estimator is fairly close to that of the PCHIP based channel estimator while others also yield error floor at high SNR values. Moreover, the performance difference between interpolation techniques increases as we consider higher modulation formats.

The BER performance results of OFDM-IM with 8-QAM and 16-QAM signaling for parameters $n = 8$, $PIR = 9$ and $N = 512$ at SNR$=$ 50 dB are given in Fig. 9 as a function of the activated subcarriers k. It

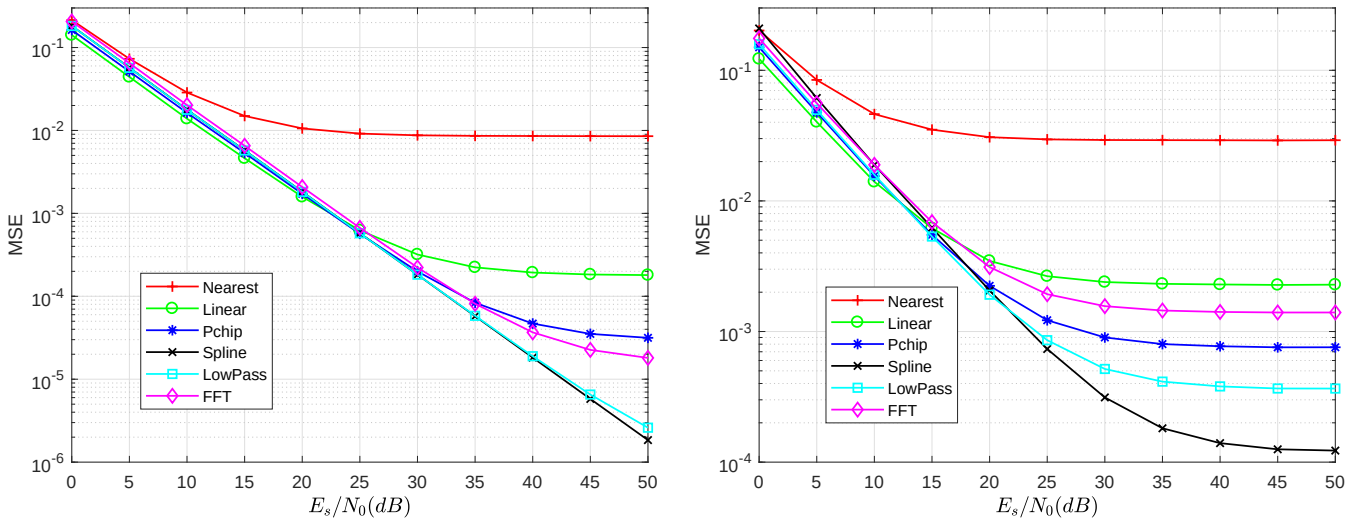

Figure 10. The MSE performance of OFDM-IM with 16QAM and $k = 2$, (a)$n = 4$, $PIR = 5$ (b)$n = 8$, $PIR = 9$

is demonstrated that the BER performance of OFDM-IM method gets worse while the total number of active subcarriers increases, in parallel with the performance of the channel estimation, which also gets worse. In particular, in Fig. 9*b*, it is observed that LPI and SPLINE have approximately a BER value of 10^{-5} while others have higher than 5×10^{-3} for $k = 5$. Consequently, LPI and SPLINE provide more than 500 times better BER value compared to the others.

The average MSE performance of proposed channel estimation methods is illustrated in Fig. 10 for OFDM-IM with parameters $k = 2$ and $N = 512$ for a wide range of SNR values. As shown in Fig. 10*a*, the MSE performance of the NI, PLI, FFTI and PCHIP are exhibit error floor at high SNR values. Moreover, the MSE performance of LPI is fairly close to SPLINE for $n = 4$, $PIR = 5$. In Fig. 10*b*, it is shown that less pilot tones (i.e, increasing PIR) causes the more MSE performance loss. As a result, the BER and MSE performance results of SPLINE and LPI based channel estimation techniques indicates that they would be better suited for the OFDM-IM system, which can be considered for next-generation wireless communication systems.

6. Conclusions

In order to detect the OFDM-IM symbols coherently, the implementation of low complexity, accurate and efficient channel estimation algorithms for OFDM-IM receivers is an important task. In this work, we have proposed a channel estimation algorithm based on interpolation for OFDM-IM systems operating over the frequency selective Rayleigh fading channel. We also demonstrated that the effects of the OFDM-IM parameters such as n, k and N on the performance of the channel estimation algorithm. It has been shown that proposed PSA-CE with LPI and SPLINE methods employed in OFDM-IM systems have superior MSE and BER performances in the presence of Rayleigh fading channel over PSA-CE with NI, PLI, FFTI and PCHIP.

Acknowledgment

The work of Y. Acar has been supported by the Scientific and Technological Research Council of Turkey (TÜBİTAK) under the BIDEB-2219 Postdoctoral Research Program. The work of E. Basar was supported by the Turkish Academy of Sciences Outstanding Young Scientist Award Programme (TÜBA-GEBİP).

References

[1] Mesleh R, Haas H, Ahn CW, Yun S. Spatial modulation - A new low complexity spectral efficiency enhancing technique. in: Proceedings Conference Communication and Networking 2006, China, pp. 1-5.

[2] Shiu DS, Foschini G, Gans M, Kahn J. Fading correlation and its effect on the capacity of multi element antenna systems. IEEE Transactions Communications, 48(3), 2000, 502-513.

[3] Loyka S, Tsoulos G, Estimating MIMO system performance using the correlation matrix approach. IEEE Communications Letter, 6(1), 2002, 19-21.

[4] Sanayei S, Nosratinia A. Antenna selection in MIMO systems. IEEE Communications Magazine, 42(10), 2004, 68-73.

[5] Basar E, Aygolu U, Panayirci E, Poor HV. Orthogonal frequency division multiplexing with index modulation. IEEE Transactions on Signal Processing, 61(22), 2013, 5536-5549.

[6] Basar E. Index Modulation Techniques for 5G Wireless Networks. IEEE Communications Magazine, 54(7), 2016, 168-175.

[7] Basar E, Wen M, Mesleh R, Di Renzo M, Xiao Y, Haas H. Index Modulation Techniques for Next-Generation Wireless Networks. IEEE Access, 5(1), 2017, 16693-16746.

[8] Acar Y, Dogan H, Panayirci E. On channel estimation for spatial modulated systems over time-varying channels. Digital Signal Processing, 37, 2015, 43-52.

[9] Acar Y, Dogan H, Basar E, Panayirci E. Interpolation based pilot-aided channel estimation for STBC spatial modulation and performance analysis under imperfect CSI. IET Communications, 10(14), 2016, 1820-1828.

[10] Acar Y, Dogan H, Panayirci E. Pilot symbol aided channel estimation for spatial modulation-OFDM systems and its performance analysis with different types of interpolations. Wireless Personal Communications, 94(3), 2017, 1387-1404.

[11] Andrews JG, Ghosh A, Muhamed R. Fundamentals of WiMAX: Understanding broadband wireless networking. Pearson Education, 2007.

[12] Dahlman E, Parkvall S, Skold J. 4G: LTE/LTE-advanced for mobile broadband, Academic press, 2013.

[13] Coleri S, Ergen M, Puri A, Bahai A. Channel estimation techniques based on pilot arrangement in OFDM systems. IEEE Transactions Broadcasting, 48(3), 2002, 223-229.

[14] Hsieh MH, Wei CH. Channel estimation for OFDM systems based on comb-type pilot arrangement in frequency selective fading channels. IEEE Transactions on Consumer Electronic, 44(1), 1998, 217-225.

[15] Dyer SA, Dyer JS. Cubic-spline interpolation 1, IEEE Instrumentation Measure Magazine. 4 (1), 2001, 44-46.

[16] Dyer S, He X. Cubic-spline interpolation: Part 2, IEEE Instrumentation Measure Magazine, 4(2), 2001, 34-36.

[17] Kahaner D, Moler C, Nash S. Numerical methods and software. Englewood Cliffs, Prentice Hall, 1989.

[18] Fritsch FN, Carlson RE. Monotone piecewise cubic interpolation. SIAM Journal of Numerical Analysis. 17(2), 1980, 238-246.

[19] Boor CD. A practical guide to splines. Springer Verlag, 1978.

[20] Coleri S, Ergen M, Puri A, Bahai A. A study of channel estimation in OFDM systems. in: Proceedings IEEE Vehicular Technology Conference, 2, 2002, pp. 894-898.

[21] IEEE Acoustics and Speech and Signal Processing Society. Digital Signal Processing Committee, Programs for digital signal processing, IEEE Press, 1979.

[22] Singhal K, Vlach J. Interpolation using the fast Fourier transform. Proceedings of the IEEE, 60(12), 1972, pp. 1558-1558.

[23] Fraser D. Interpolation by the FFT revisited-an experimental investigation. IEEE Transactions on Acoustics, Speech, and Signal Processing, 37(5), 1989, 665-675.

[24] Sipila T, Wang H. Time-domain interpolated channel estimation with noise suppression for multicarrier transmissions. in: Spread Spectrum Techniques and Applications, 2004 IEEE Eighth International Symposium on, IEEE, 2004, pp. 462-466.

[25] Xia B, Wang J. Effect of channel-estimation error on QAM systems with antenna diversity. IEEE Transaction on Communication, 52(12), 2004, 2209-2209.